RAA 2014 Vol. **14** No. **8**, 1046–1054 doi: 10.1088/1674–4527/14/8/015
http://www.raa-journal.org *http://www.iop.org/journals/raa*

Research in Astronomy and Astrophysics

Photonic lantern with multimode fibers embedded *

Hai-Jiao Yu, Qi Yan, Zong-Jun Huang, He Tian, Yu Jiang, Yong-Jun Liu, Jian-Zhong Zhang and Wei-Min Sun

Key Laboratory of In-Fiber Integrated Optics, Ministry of Education, Harbin Engineering University, Harbin 150001, China; *sunweimin@hrbeu.edu.cn*

Received 2013 March 28; accepted 2013 December 3

Abstract A photonic lantern is studied which is formed by seven multimode fibers inserted into a pure silica capillary tube. The core of the tapered end has a uniform refractive index because the polymer claddings are removed before the fibers are inserted. Consequently, the light distribution is also uniform. Two theories describing a slowly varying waveguide and multimode coupling are used to analyze the photonic lantern. The transmission loss decreases as the length of the tapered part increases. For a device with a taper length of 3.4 cm, the loss is about 1.06 dB on average for light propagating through the taper from an inserted fiber to the tapered end and 0.99 dB in the reverse direction. For a device with a taper length of 0.7 cm, the two loss values are 2.63 dB and 2.53 dB, respectively. The results show that it is possible to achieve a uniform light distribution with the tapered end and a low-loss transmission in the device if parameters related to the lantern are reasonably defined.

Key words: techniques: radial velocities — methods: laboratory — instrumentation: spectrographs

1 INTRODUCTION

Recently optical fibers have played an increasingly important role in astronomy. The technique of using fibers allows us to observe many orders of magnitude faster than to observe a single object at a time (Cvetojevic et al. 2012). The Two-degree Field Galaxy Redshift Survey (2dFGRS) uses the 2dF multi-fiber spectrograph on the Anglo-Australian Telescope, which is capable of observing 400 objects simultaneously over a 2 degree diameter field (Colless et al. 2001). The Large Sky Area Multi-Object Fiber Spectroscopic Telescope (LAMOST) currently has the highest rate of spectral acquisition. It incorporates 4000 optical fibers and opens up the ability to have large scale optical fiber spectroscopic analyzers (Wu et al. 2010; Deng et al. 2012). Through a spectral survey of millions of objects in the northern sky, LAMOST will enable research in a number of contemporary cutting edge topics in astrophysics (Zhao et al. 2012).

Besides being used to transmit a signal directly, optical fibers can also be used to make an integrated optical device that can be applied in astronomy. One of the most successful applications to date is the optical fiber image slicer (Li et al. 2009). The fibers in the slicer are arranged in a

∗ Supported by the National Natural Science Foundation of China.

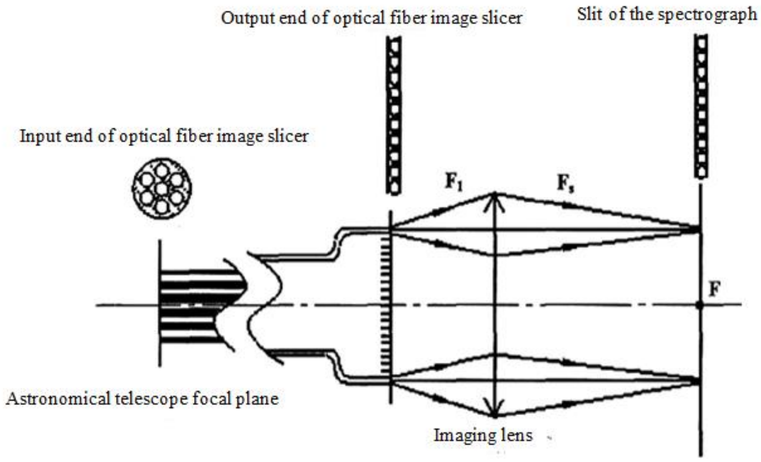

Fig. 1 A sketch of the optical fiber image slicer (Li et al. 2009).

hexagonal array at the input end, and in a linear array at the output end, as shown in Figure 1. Because of the claddings and the gaps surrounding the fibers, there are some signals that cannot be accepted by the slicer.

In this paper, a device that uses special optical fibers, which we call a “photonic lantern,” is designed to solve this problem. The diameter of the tapered end could be designed according to the demands of the telescopes. The light signal accepted by the tapered end is divided into the inserted fibers. The inserted fibers are then arranged in a line to match the entrance slit of a spectrograph.

The photonic lantern is a novel optical fiber device, which was first described by Leon-Saval et al. in 2005 and showed potential applications in astronomy. It connects singlemode fibers (SMFs) and a multimode fiber with a tapered transition. Noordegraaf et al. designed a solid all glass version with seven SMFs inserted in a low index capillary tube in 2009 (Noordegraaf et al. 2009) and with 61 SMFs in 2010 (Noordegraaf et al. 2010). In 2012, they demonstrated a photonic lantern with 19 SFM ports and a 50 μm core multimode delivery fiber (Noordegraaf et al. 2012).

All of the photonic lanterns mentioned above were designed to convert SMF ends to a multimode fiber end. Although the light propagates efficiently in these devices, there is a tendency for the light to have the highest intensity around the original cores, which can still be observed, especially at shorter wavelengths (Noordegraaf et al. 2009). The reason for this is that the embedded fibers with two different refractive indices cause a nonuniform distribution in the index of refraction, which in turn causes nonuniformity in the power intensity.

Here, we have designed a photonic lantern with a uniform refractive index in the tapered end. A length of fiber cores without polymer cladding is embedded into a silica tube. The polymer cladding can be completely removed with acetone and the silica core is kept in good condition. Before the fiber bundles are inserted into the pure silica capillary tube, the cladding of these fibers is removed. After the tapering process, the core of the tapered end has only one refractive index. The experimental results show that the light has a uniform distribution and that a low transmission loss can be realized.

Section 2 describes the theoretical analysis of the photonic lantern with multimode fibers embedded based on the slowing varying waveguide theory and multimode coupling theory. Section 3 gives the simulation results of the photonic lantern using the beam propagation method (BPM). Finally, we compared the transmission loss of the photonic lanterns with different tapers in Section 4.

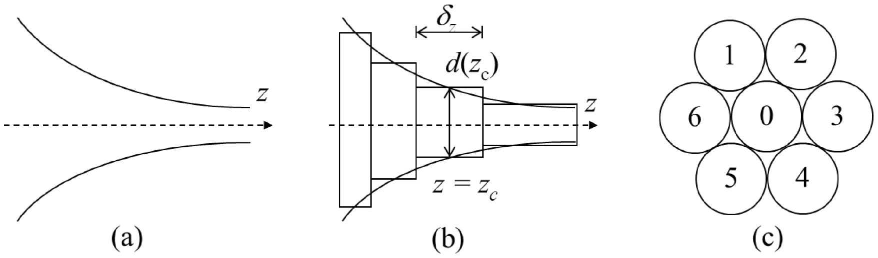

Fig. 2 Analysis of the fiber taper. (a) A slowly varying fiber with the refractive index profile $n(x, y, z)$. (b) The approximate model with z_c denoting the center of each section and z denoting the length of a particular section. (c) The cross section of a hexagonal fiber array.

2 THEORETICAL ANALYSIS

For a usual singlemode or multimode optical fiber, the optical field and the corresponding propagation constant of a guided mode can be rigorously solved. Some papers and literature (Snyder & Love 1983) have presented the necessary analytical formulas and the characteristic equations. But for the photonic lantern, the diameter along the fiber taper varies, so that the guide modes are much more complex. The model involves the slowly varying waveguide and multimode coupling. Furthermore, the two parts are closely tied to each other.

Along the direction of light propagation, the fibers have non-uniformities. If the non-uniformity changes sufficiently slowly, then the tapered part can be described by the theory of the slowly varying waveguide. The slowly varying fiber in Figure 2(a) is approximated as a series of cylindrical sections in Figure 2(b). The mode along the varying waveguide is replaced by the local mode in a certain length of the uniform cylindrical waveguide, as shown in Figure 2(b). The field of the local mode at position z_c is approximated as the mode in a fiber having infinite length with diameter $d(z_c)$ and refractive index $n(x, y, z)$. The phase and amplitude of the optical field b_{jk} depend on the coordinate z (Snyder & Love 1983)

$$b_{jk} = a_{jk}(z) e^{i \int_0^z \beta_{jk}(z) \mathrm{d}z}\,, \tag{1}$$

where j = 0, 1, 2,$\cdots$, 6 is the order of the inserted fibers as shown in Figure 2(c), k is the kth mode in the jth fiber, $a_{jk}(z)$ is the modal amplitude and $\int_0^z \beta_{jk}(z) dz$ is the phase. The field of the local mode uses an adiabatic approximation since it assumes that all changes in the profile occur over such large distances that there is a negligible change in the power of the local mode. A non-uniformity in the fiber must change over a distance that is large compared with $z_{bm} = 2\pi/|\beta_1 - \beta_2|$ (β_1 and β_2 denote the two closest propagation constants) to ensure the accuracy of the local mode solution.

Along the taper, we assume that all fibers have the same non-uniformity at a certain position. Consequently, the properties of the fibers are all the same at the same position of the taper. There is only a coupling among the same modes in the adjacent fibers. In the cross section of the taper, the fibers are in a hexagonal array, as shown in Figure 2(c). The fiber array is described by multimode coupling theory. By only considering the coupling between adjacent fibers, the center fiber is coupled with the six fibers around it and every one of these six around fibers is coupled with three neighboring fibers. However, when considering the six surrounding fibers as a whole, the coupling equations of the kth mode could be simplified

$$\frac{\mathrm{d}b_{0k}}{\mathrm{d}z} - i\beta_{0k} b_{0k} = iCB_{0k}\,, \tag{2}$$

$$\frac{\mathrm{d}B_{0k}}{\mathrm{d}z} - i\beta_{ak}B_{0k} = iCb_{0k}\,, \tag{3}$$

and

$$B_{0k} = \frac{1}{6^{1/2}}\sum_{j=1}^{6} b_{jk}\,,$$

$$C = 6^{1/2}C_{0k,1k}\,,$$

$$\beta_{ak} = \beta_{1k} + 2C_{1k,2k}\,,$$

where $C_{0k,1k}$ is the coupling coefficient between fiber 0 and fiber 1, and C is the coupling coefficient between fiber 0 and all of the other fibers around it. β_{0k} and β_{1k} are the propagation constants of the center fiber and the surrounding fibers. Since all of the fibers are the same, $C_{0k,1k} = C_{1k,2k}$ and $\beta_{0k} = \beta_{1k}$.

The coupling equations are similar to those which represent the cross coupling of two fibers. Consequently, the fiber array could be analyzed as two different fibers.

The coupling coefficients of two fiber modes are expressed as (Snyder & Love 1983)

$$C_{jk}(z) = C_{kj}(z) \cong \frac{1}{4}\frac{W}{N_j}\left(\frac{\varepsilon_0}{\mu_0}\right)^{1/2}\int_{S_\infty}(n^2 - n_j^2)\psi_j\psi_k\mathrm{d}S\,, \tag{4}$$

where $N_j = (n_{\rm core}/2)(\varepsilon_0/\mu_0)^{1/2}|\int_{S_\infty}(\psi^2 dA)|$ is defined as mode normalization related to the normalized frequency V, $W = 2\pi/\lambda$ is the wavenumber, ψ_j is the solution of the scalar wave equation for the jth fiber in isolation and n is the refractive index of the composite waveguide, i.e. $n = n_{\rm core}$ over the cores and $n = n_{\rm cladding}$ elsewhere. According to Equation (1), N_j, ψ_j and n depend on z, thus the coupling coefficient also depends on z. In our lantern, the central and surrounding fibers are identical, so all of the coupling coefficients are the same. For the two identical fibers with the step refractive index, we can determine the coupling coefficient using the Gaussian approximation for the fundamental modes. Replacing ψ_j and ψ_k with the Gaussian near-field and far-field approximation equations respectively, we derive an expression for C

$$C = \frac{1}{\rho}\left(\frac{\Delta}{\pi A}\right)^{1/2}\frac{V^3\ln V}{(V^2-1)(V-1)^{1/2}}\exp\left[(V-1)\left(\frac{V}{V+1} - A\right)\right], \tag{5}$$

where $A = d/\rho$ is the relative separation of the fibers, ρ is the radius for the core of the optical fiber, $V = k\rho n_{\rm core}\sqrt{2\Delta}$ is the normalized frequency and $\Delta = (n^2_{\rm core} - n^2_{\rm cladding})/2n^2_{\rm core}$ is the relative refractive index difference. The normalized coefficient $\lg[\rho C/\Delta^{1/2}]$ is plotted as a function V for various A in Figure 3, and as a function of A for various V in Figure 4.

For a certain V, the value of the normalized coefficient decreases exponentially with increasing distance as the mode fields further overlap. The same variation in the relative separation will lead to a larger change of the coupling coefficient for a fiber with larger V. Consequently, it is accurate and simple to ignore all but the adjacent coupling in an array of fibers with a large core. For fixed distance, the coefficient increases exponentially with decreasing V as more mode power spreads into the cladding around the fibers. The wider the relative separation is, the more sensitive the coupling coefficient with V will be. The decreased diameter and separation of the fibers would result in a high degree of modes cross-coupling in each fiber, inducing lower order modes that couple to higher order modes.

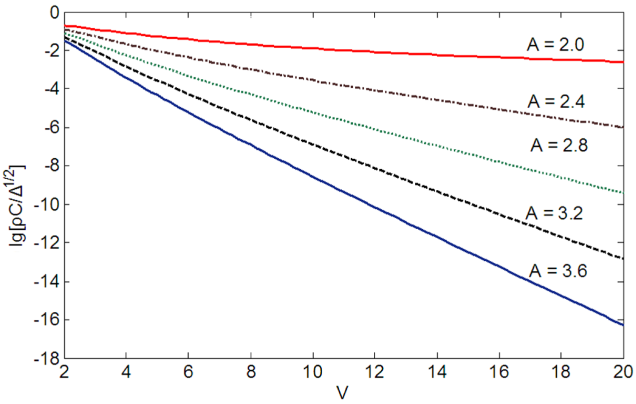

Fig. 3 The normalized coefficient $\lg[\rho C/\Delta^{1/2}]$ vs. V for various A.

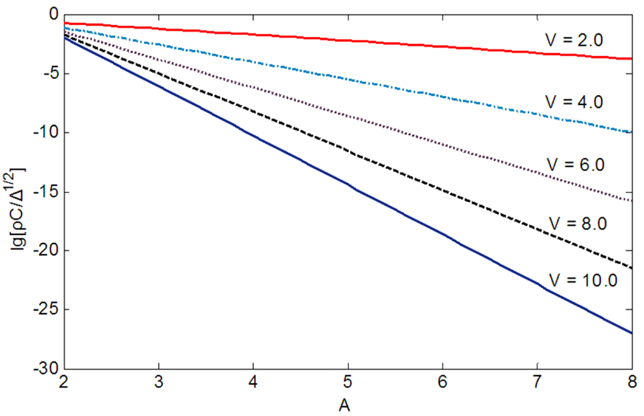

Fig. 4 The normalized coefficient $\lg[\rho C/\Delta^{1/2}]$ vs. A for various V.

3 SIMULATION RESULTS

The BPM is one of the most widely used analysis methods for photonic devices. The distribution of light power along the z direction is shown in Figure 5. Some mathematical models could be used to describe the actual shape of the taper (Albandakji et al. 2006). In our simulation the shape of the taper is approximated as a cosine S-bend shape, which is similar to the actual shape. z_0 and z_1 are z coordinates of the starting and ending position of the taper. The other parameters are as follows: the large-core fibers are chosen as the bare optical fibers with a core diameter of 90 μm and a refractive index of 1.46; the outer diameter of the silica capillary tube is 600 μm and the refractive index is 1.4575; the input of the photonic lantern is from the embedded fiber array with a Gaussian beam distribution; the wavelength is 0.632 μm in the range of visible light; a draw ratio of 4 for the diameter is selected for the taper.

Due to the geometrical symmetry of the lantern, we choose the left and middle embedded fibers in Figure 5(b) for monitoring. The energy along the embedded fibers is shown in Figure 5(c)∼(e) corresponding to the different lengths of the taper, 3.0×10^4, 3.5×10^4 and 4.0×10^4 μm respectively. From the analysis in Figures 3 and 4, the relative separations A and the variation of the normalized frequency V simultaneously affect the coupling coefficient. At the beginning of the taper, although

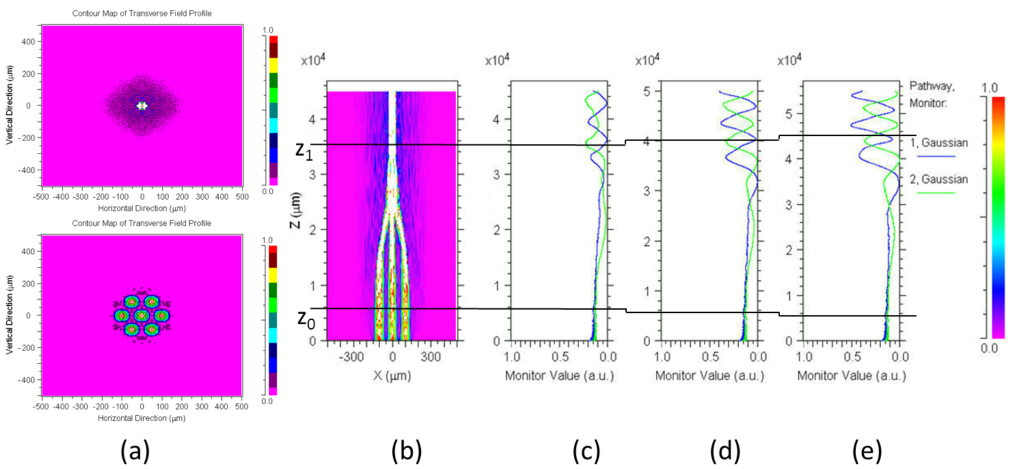

Fig. 5 The simulation results of the tapered fiber. (a) The cross sections of the separated fibers (*bottom*) and the tapered end (*top*) of the lantern. (b) The energy distribution along the lantern at the profile $y = 0$. (c) $\sim$(e) are values for the monitored power that correspond to different lengths of the taper, 3.0×10^4, 3.5×10^4 and 4.0×10^4 μm respectively. The wavelength is 632.8 nm. The blue and green lines represent the light power in the middle and left cores in (b) respectively.

the fibers are close, V is so large that it leads to a small coupling coefficient. The power in different fibers exchanges little (the bottom in Figure 5(a)). When the taper is thinner, V and A are smaller, and the coupling effect is greater. At the tapered end, the power mixes in the core of the multimode waveguide which is formed by fusing and tapering (the top in Fig. 5(a)).

According to the theory of a slowly varying waveguide, the length of the taper influences the loss in the device. As shown in Figure 5(c)$\sim$(e) when the length of the taper is only 3.0×10^4 μm, there is more power lost in the tapered end. The longer the taper is, the slower the variation in the diameter will be, and the more the power is confined in the device. Because there is a difference between the model used in the simulation and the actual device, we cannot give an accurate quantitative conclusion of the transmission loss, but we can give a qualitative conclusion. The corollary of the simulation results is that lengthening the taper could lead to a low loss. We made some tapers to demonstrate this trend.

4 EXPERIMENTAL RESULTS

Technically, it is hard to control the shape of the taper of a fiber preform by using existing equipment, so we designed and built a taper system with a large heating zone and a moving planner flame. Some samples of lanterns were fabricated using this tapering machine.

After analyzing some samples with SMFs embedded, we chose a special large-core fiber with polymer cladding as the inserted fiber. After removing the polymer cladding, we inserted the fiber cores inside a silica tube, and then fabricated the lantern. The diameter of the core was 125 μm. The index of the embedded fiber cores was higher than the index of the silica tube.

In order to further verify the simulation result that the transmission loss decreases with a longer taper, we chose two devices for comparison. One has a taper length of 3.4 cm, and the other has a taper length of 0.7 cm. In the tapered end, both of the lanterns have a core diameter of about 100 μm and a cladding diameter of about 250 μm. We took a series of photos of segments of the

Table 1 The Transmission Loss from an Inserted Fiber Port to the Tapered End (taper length = 3.4 cm)

Fiber port	P_{in} (µW)	P_{out} (µW)	Loss (dB)
a	47	37	1.04
b	46	32	1.58
c	46	37	0.94
d	47	39	0.81
e	46	35	1.19
f	46	37	0.94
g	45	34	1.22
Average	–	–	1.06

Table 2 Same as Table 1, but for taper length = 0.7 cm

Fiber port	P_{in} (µW)	P_{out} (µW)	Loss (dB)
a	46	22	3.20
b	44	22	3.01
c	48	23	3.19
d	47	29	2.10
e	34	16	3.27
f	39	25	1.93
g	34	23	1.70
Average	–	–	2.63

lantern with a longer taper using microscopy, as shown in Figure 6(a), because the whole lantern is not easily shown in one picture. In the first part of the taper, the cores become thinner and closer but they are still separated. In the final part, the cores and the tube are fused together. The cores of the embedded fibers no longer act as individuals and are fused to form a new uniform core, as shown in Figure 6(b). The silica tube becomes the new cladding. The near-field image of the tapered end is shown in Figure 6(c), with an inserted fiber illuminated by white light. The bright tilted edge is the trace left by a cleaver after cutting. The near-field images are almost the same no matter which embedded fiber is illuminated. The power of the light is confined to the core and the power distribution in the core is uniform.

First, the transmission loss from an inserted fiber port to the tapered end is measured and is then also measured in the opposite direction. Figure 7 shows the sketch of the setup used for the experiment. To measure the transmission loss, seven delivery fibers are fused with a separate inserted fiber port. The delivery fibers are the same as the inserted fiber, so that the loss from the fusing process can be ignored. The 632.8 µm laser light was focused into one of the delivery fibers and the output was monitored from the tapered end, as shown in Figure 7(a). Hence, the transmission loss in the lantern could be calculated as

$$\text{Loss} = 10\,\text{lg}(P_{\text{in}}/P_{\text{out}})\,, \tag{6}$$

where P_{in} is the value of input power and P_{out} is the value of output power.

The laser light is sent to the seven inserted fibers and the loss is tested in the same way. The test results are shown in Tables 1 and 2. The average transmission loss of the longer device is 1.06 dB and that of the shorter one is 2.63 dB.

The transmission loss from the tapered end to the seven inserted fibers is also measured. The setup is shown in Figure 7(b). Since it is hard to fuse the tapered end with the fiber, the delivery fiber and the tapered end are face to face, with a separation of about 100 µm (Fig. 7(b)). In order to reduce the coupling loss, an SMF that has a smaller far field divergence angle is chosen as the delivery fiber. The loss is calculated with Equation (6). Here, P_{in} is the power of the SMF output and P_{out} is the

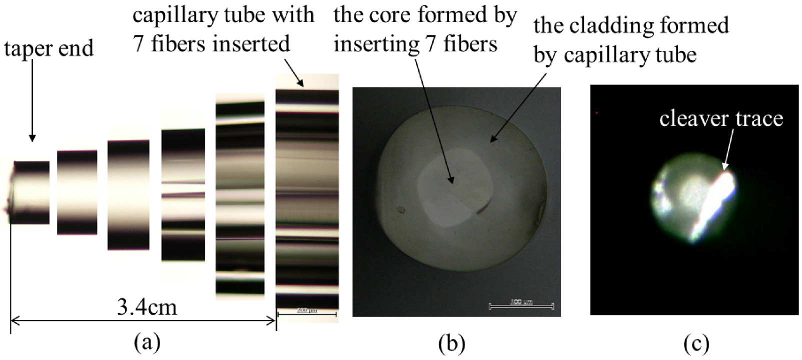

Fig. 6 (a) Pictures of segments in the photonic lantern. (b) Microscopic picture of the tapered end in (a). (c) The near-field image of the taper with incident white light.

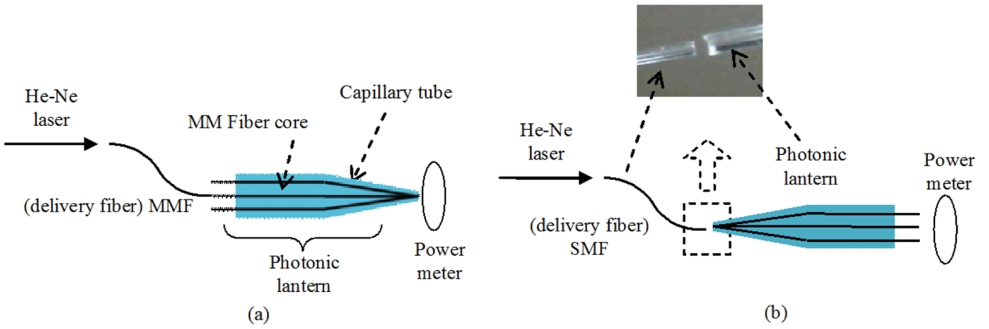

Fig. 7 The setup for measurement of loss from an inserted fiber port to the tapered end (a) and in the reverse direction (b).

Table 3 The Transmission Loss from the Tapered End to the Seven Embedded Fiber Ports (taper length = 3.4 cm)

Fiber port	P_{out} (μW)	P_{in} (μW)	Loss (dB)
a	0.12		
b	0.09		
c	0.15		
d	0.15	–	–
e	0.11		
f	0.14		
g	0.10		
Sum	0.86	1.08	0.99

total power of the seven embedded fibers. The measured results are shown in Tables 3 and 4. The loss includes the transmission loss of the device and the coupling loss. The transmission loss of the longer device is 0.99 dB and that for the shorter one is 2.53 dB.

Table 4 Same as Table 3, but for taper length = 0.7 cm

Fiber port	$P_{\rm out}$ (μW)	$P_{\rm in}$ (μW)	Loss (dB)
a	0.10		
b	0.11		
c	0.09		
d	0.09	–	–
e	0.12		
f	0.07		
g	0.13		
Sum	0.71	1.27	2.53

Comparing the test results of the two devices, it is clear that the length of the taper influences the transmission loss of the device. Lengthening the taper could reduce the transmission loss. However, the loss of the device with a 3.4 cm taper length is not low enough. One reason for this may be that the length of the taper is still not sufficiently long enough. Another reason may be that the core of the tapered end does not have a regular shape (Fig. 7(b)) due to inhomogeneous heating in the tapering process.

5 CONCLUSIONS

A photonic lantern with multimode embedded fibers was able to achieve a uniform power distribution at the tapered end and somewhat low-loss transmission. Both the simulation and the test results show that the transmission loss decreases with a longer length of the taper. Consequently, it is possible to simultaneously get a uniform index profile in the tapered end and a low loss during transmission.

Acknowledgements This work is supported by the National Natural Science Foundation of China (Grant Nos. 11078009, U1331114, 61107059 and 61307076), the 111 project (B13015) to Harbin Engineering University, the Fundamental Research Funds for the Central Universities, and the Opening Project of Key Laboratory of Astronomical Optics and Technology, Nanjing Institute of Astronomical Optics and Technology, Chinese Academy of Sciences.

References

Albandakji, M. R., Safaai-Jazi, A., & Stolen, R. H. 2006, in Proc. SPIE 6369, Photonic Crystals and Photonic Crystal Fibers for Sensing Applications II, 6369, 636902 (International Society for Optics and Photonics)

Colless, M., Dalton, G., Maddox, S., et al. 2001, MNRAS, 328, 1039

Cvetojevic, N., Jovanovic, N., Lawrence, J., Withford, M. & Bland-Hawthorn, J., 2012, Optical Express, 20, 2062

Deng, L.-C., Newberg, H. J., Liu, C., et al. 2012, RAA (Research in Astronomy and Astrophysics), 12, 735

Leon-Saval, S. G., Birks, T. A., Bland-Hawthorn, J., & Englund, M. 2005, Optics Letters, 30, 2545

Li, L.-B., Zhu, Y.-T., & Hu, Z.-W. 2009, Astronomical Research & Technology, 6, 220

Noordegraaf, D., Skovgaard, P. M., Nielsen, M. D., & Bland-Hawthorn, J. 2009, Optics Express, 17, 1988

Noordegraaf, D., Skovgaard, P. M. W., Maack, M. D., et al. 2010, in Proc. SPIE 7580, Fiber Lasers VII: Technology, Systems, and Applications, 75802D (International Society for Optics and Photonics)

Noordegraaf, D., Skovgaard, P. M. W., Sandberg, R. H., et al. 2012, Optics Letters, 37, 452

Snyder, A. W., & Love, J. D. 1983, Optical Waveguide Theory (London: Chapman and Hall)

Wu, X.-B., Jia, Z.-D., Chen, Z.-Y., et al. 2010, RAA (Research in Astronomy and Astrophysics), 10, 745

Zhao, G., Zhao, Y.-H., Chu, Y.-Q., Jing, Y.-P., & Deng, L.-C. 2012, RAA (Research in Astronomy and Astrophysics), 12, 723